arXiv:chao-dyn/9810027v2 25 May 1999

Homoclinic Structure Controls Chaotic Tunnelling

Stephen C. Creagh[a,b†] and Niall D. Whelan[a,c]
[a] *Division de Physique Théorique*, Institut de Physique Nucléaire 91406, Orsay CEDEX, France.*
[b] *Service de Physique Théorique,CEA/Saclay, 91191, Gif-sur-Yvette CEDEX, France.*
[c] *Department of Physics and Astronomy, McMaster University, Hamilton, Ontario, Canada L8S 4M1.*
(June 8, 2007)

Tunnelling from a chaotic potential well is explained in terms of a set of complex periodic orbits which contain information about the real dynamics inside the well as well as the complex dynamics under the confining barrier. These orbits are associated with trajectories which are homoclinic to a real trajectory emerging from the optimal tunnelling path. The theory is verified by considering a model double-well problem.

PACS numbers: 03.65.Sq, 73.40Gk, 05.45.Mt, 05.45.-a

Chaos is ubiquitous in nature. For this reason, its effect on quantum systems is very well studied [1] and powerful semiclassical techniques have been developed to treat it. However, tunnelling has largely remained impervious to such analysis. We show that a simple principle underlies the detailed behaviour of tunnelling in chaotic systems — state to state fluctuations in the tunnelling rate are determined by a restricted set of complex classical trajectories which can be constructed straightforwardly using known techniques of dynamical systems.

Previous analyses of chaotic tunnelling exist in contexts where a quantum state is initially localised in an integrable region of phase space and tunnels into or through a chaotic region [2,3]. Our goal is different; we consider systems that are almost completely chaotic and tunnelling is through an energetic barrier. We then construct a periodic-orbit theory of tunnelling analogous to Gutzwiller's celebrated formula for the density of states. It relates tunnelling rates to a set of complex classical trajectories which can be understood intuitively as follows. In any potential barrier, there is an optimal tunnelling route determined by a complex trajectory with minimal imaginary action. Interference effects in the tunnelling rate are produced by trajectories which originate from and return to a small region of phase space surrounding the minimal trajectory. In chaotic systems, such recurrent trajectories are understood on the basis of "homoclinic intersections". Technical details come later, but the main point is that such trajectories are standard in dynamical systems theory and are relatively easy to find. These orbits dominate tunnelling rates in a manner similar to the way in which they control wavepacket recurrences as discovered in [4]. See also [5].

We treat double well potentials for which $V(-x,y) = V(x,y)$ and examine the energy level splittings of quasi-degenerate doublets labelled by n (although our general conclusions apply equally to resonances in metastable wells [6,7]). Detailed numerical calculation will be for $V(x,y) = (x^2-1)^4 + x^2y^2 + \mu y^2$ with $\mu = 1/10$. It will prove useful, instead of dealing directly with the energy-level spectrum, to regard $q = 1/\hbar$ as a parameter and ask for the values q_n for which a given energy E is an eigenvalue — this leads to calculations with a fixed classical dynamics. We then obtain doublets at values q_n with splittings Δq_n between them. We investigate tunnelling by constructing the function [8],

$$f(q) = \sum \Delta q_n \delta(q - q_n). \tag{1}$$

The spectrum and tunnelling splittings are encoded in $f(q)$. Semiclassically, it can be approximated as a sum over *pseudoperiodic* orbits which start on one side of the energy barrier and, after evolution in complex time, finish at the symmetric image of the initial point. In [8] it was shown that when the optimal tunnelling route is along a symmetry axis, a quasi-periodic oscillation arises in the tunnelling rate which is related to the action of a real periodic orbit, also on the symmetry axis. However, there remain significant fluctuations which we now explain using non-axial orbits homoclinic to this real orbit.

We can visualise a complex pseudoperiodic orbit as a one-dimensional path in complex phase space. However, it is not unique — it corresponds to a given contour describing its complex time evolution; any deformation of this contour gives an equivalent orbit. Because of this freedom, a systematic and unambiguous description is difficult if we work in full phase space. The situation simplifies considerably if we restrict dynamics to a surface of section. Pseudoperiodic orbits then reduce to single, isolated points of intersection with the surface of section and classification of them is simpler. An added advantage is that metastable sytems can be treated within the same formalism [6,10].

Let Σ denote a surface of section through one of the wells, defined in the usual manner of real dynamics (eg. $x = x_0$, $\dot{x} > 0$ and $H = E$.) Let $F : \Sigma \to \Sigma$ denote the first return surface of section mapping, defined by letting trajectories start on Σ and evolve under real dynamics until they intersect Σ once again. Real periodic orbits correspond to fixed points of some iterate F^r of F. We incorporate tunnelling by introducing a second *complex* map $\mathcal{F}$ acting on the same section Σ as follows.

Any potential barrier has an orbit γ_0 which crosses

it with minimum imaginary action iK_0 in an imaginary time $-i\tau_0$. It evolves in complex phase space except at two turning points where it is fully real. There is a real point z_0 on Σ which evolves to one of these endpoints under real time evolution. It has a symmetric image σz_0 on $\sigma\Sigma$ which evolves to the other endpoint. (Here σ refers to the symmetry operation — reflection in x in our example.) The point z_0 evolves into σz_0 if we integrate along a complex time contour C as follows: first the contour evolves along the real axis until the trajectory reaches the turning point of γ_0, then it descends parallel to the imaginary axis until the turning point on the other side of the barrier is reached and finally retraces the evolution parallel to the real axis (in negative real time) until σz_0 is reached. The net time of evolution is $-i\tau_0$.

We define the map $\mathcal{F}$ by deforming γ_0. If a point z' near z_0 is chosen on Σ, a deformation of C can be found such that the final point z'' is on $\sigma\Sigma$. By invoking the symmetry operation to map $\sigma\Sigma$ back to Σ, we define a complex symplectic map $\mathcal{F} : z' \mapsto z = \sigma^{-1}z''$ from Σ onto itself. The central orbit γ_0 corresponds to a real fixed point z_0 of $\mathcal{F}$ while other initial conditions, even if real, are mapped to complex images under $\mathcal{F}$. Just as the real periodic orbits give real fixed points of F^r, the complex pseudoperiodic orbits give complex fixed points of $\mathcal{F}F^r$; such fixed points define orbits with r oscillations in one well before tunnelling across the barrier.

Following [9], the classical maps F and $\mathcal{F}$ have quantisations [6] as unitary and hermitean operators, respectively, acting on a Hilbert space which quantises Σ. The expression for $f(q)$ as a sum over the fixed points of $\mathcal{F}F^r$ has an interpretation as a sum over traces of such operators, as will be shown in a future publication [10]. Neglecting multiple tunnelling traversals and the uniform analysis needed at the bottom and top of the wells,

$$f(q) \approx f_0(q) + \frac{2}{\pi}\,\mathrm{Re}\sum_{r=1}^{\infty}\sum_{\gamma\in P_r} A_\gamma e^{iqS_\gamma}, \qquad (2)$$

where P_r denotes the set of fixed points of $\mathcal{F}F^r$. The $f_0(q)$ term is determined by γ_0, is monotonic and gives the average behaviour of the splittings [8]. The contributions with $r \geq 1$ have complex actions S_γ with nonzero real parts and describe fluctuations superimposed on $f_0(q)$. The amplitudes are $A_\gamma = 1/\sqrt{-\det(M_\gamma - I)}$ where M_γ is the complex 2×2 symplectic matrix linearising $\mathcal{F}F^r$ about γ (note that a different phase convention was used in [8].) The choice of root in A_γ can be unambiguously assigned using the real dynamics [10].

In problems with an additional symmetry axis (for us it is along $y = 0$), the point z_0 is a fixed point of both $\mathcal{F}$ *and* F and thus of each $\mathcal{F}F^r$. The treatment in [8] consisted of treating only this fixed point in each of the terms in (2). We now systematically include the other fixed points, which are generally complex.

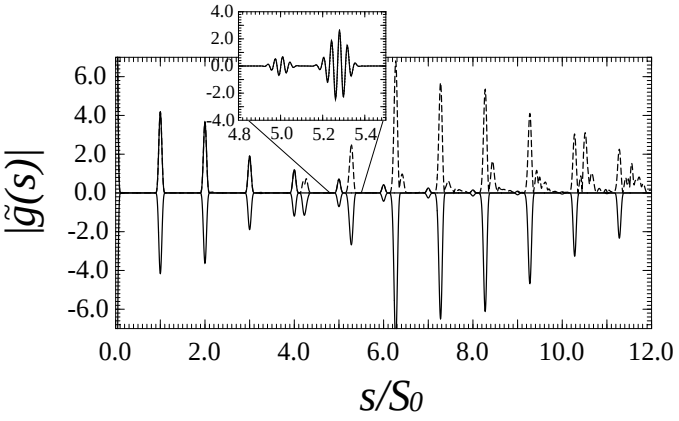

FIG. 1. Dashed curve: Fourier transform of $g(q)$ obtained quantum mechanically. Upper solid curve: semiclassical prediction using just the axial orbits. Lower solid curve: theory, using the six homoclinic families shown in Fig. 2. Inset: the quantum-mechanical $\mathrm{Re}\,\tilde{g}(s)$ and the semiclassical prediction in a limited range (note there are two superimposed curves). Peaks not accounted for by the lower curve correspond to uncomputed secondary intersections.

We now scale out the smooth exponential variation with q by defining $g(q) = f(q)/f_0(q)$ which is a function of order unity. It is the same as Eq. (1) but with Δq_n replaced by $x_n = \Delta q_n/f_0(q_n)$. We find

$$g(q) = 1 + \mathrm{Re}\sum_{r=1}^{\infty}\sum_{\gamma\in P_r} A'_\gamma e^{iq(S_\gamma - iK_0)} \qquad (3)$$

where A'_γ is the rescaled amplitude. Note that q only appears in the exponents and that the residual action $S_\gamma - iK_0$ is predominantly real if $\mathrm{Im}\,S_\gamma \approx K_0$ so that $g(q)$ is an oscillatory function.

In Fig. 1 we show the Fourier transform $\tilde{g}(s)$ of $g(q)$ for energy $E = 0.9$ and $q \in [30, 100]$, chosen to put us well within the semiclassical regime. For each r, the fixed point of $\mathcal{F}F^r$ at z_0 has action $S_\gamma = rS_0 + iK_0$, where S_0 is the action of the on axis real periodic orbit in one of the wells. Therefore $\tilde{g}(s)$ exhibits a series of simple peaks at the harmonics $s = rS_0$, well reproduced by the semiclassical theory. More interesting is the additional structure, primarily in the form of a sequence of regularly spaced peaks shifted away from the simple harmonics, which we now explain using nonaxial orbits.

Among barrier-crossing orbits, the minimum imaginary action is that of γ_0; the contributions of other orbits are suppressed by order $\exp(-\Delta K/\hbar)$ where ΔK is the additional imaginary action. To be numerically significant, orbits in the sum Eq. (3) should have a small ΔK and so should begin and end near z_0. On the other hand, to contain information about the entire spectrum as implied in (1), they should fully explore the phase space. These two requirements are satisfied by trajectories homoclinic to z_0. Asymptotically, these trajectories

approach z_0 under both forward and backward time evolution as $d(t) \sim e^{-\nu|t|}$, where ν is the stability exponent of the central orbit and t counts intersections with the Poincaré section. In practice they are easily calculated as the intersections of the stable and unstable manifolds of z_0 (the sets of points in phase space which approach z_0 under forward and backward time evolution, respectively.) For a general discussion see [11].

Let $(\cdots x_{-2}, x_{-1}, x_0, x_1, x_2 \cdots)$ be the intersection of one such trajectory with Σ. Then a truncation $(x_{-M} \cdots x_{-1}, x_0, x_1, \cdots, x_N)$ is a finite length trajectory which is almost a periodic orbit if M and N are large because x_{-M} and x_N are exponentially close to z_0 and to each other. By slightly perturbing the initial condition, one can find a nearby fixed point of $\mathcal{F}F^r$, where $r = M + N$, by complex Newton iteration. The tunnelling segment of this trajectory is very close to γ_0 and as a result the imaginary part of the action is close to the optimal value K_0. In the trace formula, there is then a competition of exponentials — the imaginary part of the action will decay exponentially with length according to $\mathrm{Im}(S_\gamma - iK_0) \sim e^{-\nu \min(M,N)}$ and this can be smaller than $\hbar$ so that $e^{-q(S_\gamma - iK_0)}$ is nonnegligeable. For a fixed r, each choice of M (and $N = r - M$) gives a distinct fixed point although only a subset will be numerically significant (the effective number depends on q and is given by the criterion that $\mathrm{Im}(S_\gamma - iK_0) \sim e^{-\nu \min(M,N)} \lesssim \hbar$). While the arguments above are asymptotic in M and N, in practice complex orbits could usually be found as long as $M, N > 2$ for the system we examine.

The near equal spacing of the peaks is because one extra iteration of the real map amounts to including one extra F-bounce near z_0; to a good approximation this adds S_0 to the action. Also note that the homoclinic peaks are larger than the peaks at $s = rS_0$ beyond about $r = 5$. Each homoclinic peak actually contains the contribution of many fixed points, all with approximately the same action. This quasidegeneracy is because there is more than one homoclinic trajectory and because of the choice of M for a given r as explained above. The amplitude of any single orbit initially grows algebraically with length due to the increasing quasidegeneracy of the orbit. This is ultimately overcome by the exponential decay with length due to the instability of long orbits. In this case the maximum is around $r = 7$. There is additional structure which dominates at larger r and which we ascribe to secondary homoclinic intersections. This scenario is like the calculation of wavefunction recurrences in [4], where there is also a selection of trajectories which return to a classically small region of phase space. There the region is determined by a Gaussian wavepacket, whereas here it is by the near-Gaussian kernel of an operator quantising $\mathcal{F}$ [6,10]. Fourier analysis reveals peak structure similarly organised around homoclinic orbits [4,12].

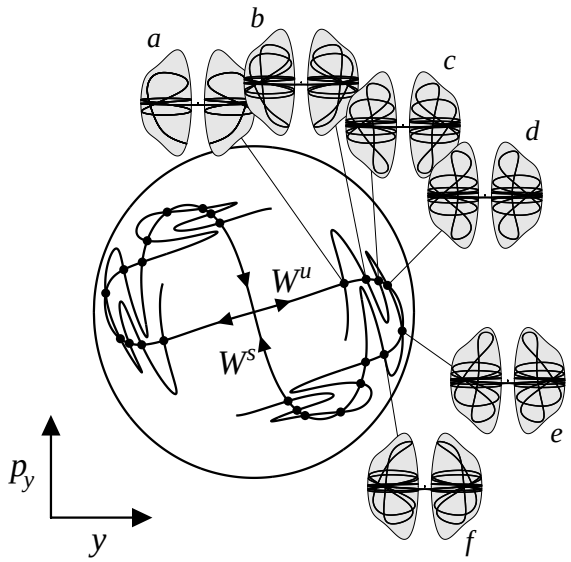

FIG. 2. The surface of section defined by $E = 0.9$ and $x = 0.6$. The circle is the boundary of the energetically allowed region. W^u and W^s are the stable and unstable manifolds whose intersections define the homoclinic trajectories: the six distinct ones being labelled a to f. For each one, we show the trajectory in configuration space of a corresponding tunnelling orbit. Actually shown is the full periodic orbit which is the double iteration of the pseudoperiodic orbit used in calculation. Also, only the real parts are shown; the small imaginary components being too small to see.

We now apply this formalism to the potential $V(x, y)$. Shown in Fig. 2 are the stable and unstable manifolds of z_0 in the $x = 0.6$ surface of section. Of particular interest is a sequence of 6 primary intersections labelled a to f. (All other intersections shown are either iterates of these six or are related by reflection in y and p_y.) This is a rather rich structure; often there are only 2 primary intersections [11]. Each of these intersections defines a homoclinic trajectory, and a corresponding series of fixed points of $\mathcal{F}F^r$. We show the projections in real configuration space of complex trajectories defined for each of these intersections by the truncation $(M, N) = (3, 5)$ corresponding to the peak at $s \approx 8.2S_0$.

The symmetries of time-reversal and reflection in y lead to degeneracy among the orbits. The families b and c are respectively mapped into those of f and e under a combination of the two symmetries. Congruent but distinct families are obtained if we apply either symmetry alone. The family a maps to itself under time-reversal but a distinct family is obtained under reflection in y, while the converse applies to d. We therefore only have four inequivalent families: a, b, c and d with degeneracies 2, 4, 4 and 2 respectively. This high degeneracy (including also the choice M), compared to the single axial orbit, is responsible for the relative dominance of the associated peaks in Fig. 1. In the resolution presently available, the individual contributions of $\{a, b, c, d\}$ are not resolved,

but presumably would be with a wider q-window.

To get detailed agreement in Fig. 1 we had to include a family of "ghost" orbits in addition to the orbits described above. Near the intersections a and b, there is a switchback in the stable manifold emanating from f that almost produces two additional intersections; at lower energies these intersections actually occur and lead to two new families of orbits. These can be tracked up to $E = 0.9$, although they become complex. (These orbits are analogous to the ghost orbits of [13].) One of them is exponentially large and is excluded through the Stokes phenomenon. The other does contribute and is an important component in the leading edges of the peaks. The Fourier transform is then almost completely reproduced up to about $s = 8S_0$. Thereafter additional side peaks emerge which can be explained by the secondary intersections (which would be seen in Fig. 2 if the invariant manifolds were extended.) Therefore, a systematic calculation of homoclinic structure suffices for a complete understanding of chaotic tunnelling.

While the details presented here are limited to systems with additional symmetry in y, we claim that the guiding principle applies generally. If the real extension of γ_0 is not periodic, the tunnelling is given by trajectories homoclinic to it, though they are not as simply organised as here. The important physical notion is that homoclinic trajectories are asymptotic to the optimal tunnelling route while fully exploring classical phase space.

There has been significant recent effort to understand dynamical tunnelling in which the barriers are not energetic but come from dynamical effects such as KAM surfaces [2,3]. In particular, an exhaustive semiclassical analysis was carried out for one particular system in [3]. The authors considered the propagation of a quantum state initially localised in a regular region of phase space and used complex trajectories to describe its penetration into a chaotic region. Explicit semiclassical formulas were developed but it is difficult to make a direct comparison to our results. Here we have considered a purely spectral quantity in terms of classical invariants — the complex periodic orbits — while they considered the propagation of a specific quantum state. In terms of the quantities considered, namely splittings, the work of [2] is closer in spirit. However, because of the complicated, mixed nature of the phase space, there are no explicit semiclassical results of the type derived here. In particular, the splittings typically vary over many orders of magnitude, even after normalisation by the local mean, unlike what we observe. While it would be desireable to develop an explicit semiclassical formalism for such systems, it is far from obvious how this could be done.

The problem of the statistics of the normalised splittings will be addressed in a later publication [10]. For now we remark that they are not governed by the Porter-Thomas distribution but depend on the specific properties of γ_0. This is in spite of the fact that splittings are formally similar to resonance widths for which one expects Porter-Thomas [14]. This effect is quite general and should also apply to certain resonance problems.

---

† Present address: Division of Theoretical Mechanics, School of Mathematical Sciences, University of Nottingham, NG7 2RD, UK.

* Unité de recherche des Universités de Paris XI et Paris VI associée au CNRS.

[1] M. C. Gutzwiller, *Chaos in Classical and Quantum Mechanics* (Springer Verlag, New York, 1990).

[2] W. A. Lin and L. E. Ballentine, Phys. Rev. Lett. **65**, 2927 (1990); O. Bohigas, S. Tomsovic and D. Ullmo, Phys. Rev. Lett. **64**, 1479 (1990); Phys. Rep. **223**, 45 (1993); O. Bohigas et al., Nucl. Phys. **A560**, 197 (1993); S. Tomsovic and D. Ullmo, Phys. Rev. E **50**, 145 (1994). E. Doron and S. D. Frischat, Phys. Rev. Lett. **75**, 3661 (1995); Phy. Rev. E **57**, 1421 (1998).

[3] A. Shudo and K. Ikeda, Prog. Theor. Phys. Supplement No. 116, 283 (1994); Phys. Rev. Lett. **74**, 682 (1995); *ibid.* **76**, 4151 (1996); Physica D **115**, 234 (1998).

[4] S. Tomsovic and E. J. Heller, Phys. Rev. E **47**, 282 (1993).

[5] A. Ozorio de Almeida, Nonlinearity **2**, 519 (1989).

[6] S. C. Creagh and N. D. Whelan, Ann. Phys. **272**, 196 (1999).

[7] M. W. Beims, V. Kondratovich and J. B. Delos, Phys. Rev. Lett. **81**, 4537 (1998).

[8] S. C. Creagh and N. D. Whelan, Phys. Rev. Lett. **77**, 4975 (1996).

[9] E. B. Bogomolny, Nonlinearity **5**, 805 (1992).

[10] S. C. Creagh and N. D. Whelan, to appear.

[11] S. Wiggins, *Chaotic Transport in Dynamical Systems*, Springer-Verlag, New York (1992).

[12] K. Hirai and E. J. Heller, Phys. Rev. Lett. **79**, 1249 (1997).

[13] M. Kus, F. Haake and D. Delande, Phys. Rev. Lett. **71** 2167 (1993).

[14] C. E. Porter (ed.), *Statistical Theory of Spectra*, Academic Press, New York (1965).